ISSN 2462-2052 | eISSN 2600-8718 *Journal of Science and Mathematics Letters*
DOI: https://doi.org/10.37134/jsml.vol13.2.8.2025 *Volume 13, Issue 2, 107-119, 2025*

Research Article

Synthesis and Evaluation of Alkoxy-Substituted Thiourea Derivatives as Antifouling Agents in Marine Ecosystem Interests

Wan M. Khairul[1*], Adibah Izzati Daud[2], Sze Ee Sylvia Voon[1], Chiong Hwee Hii[1], Noraznawati Ismail[3] and Mauricio F. Erben[4]

[1]Faculty of Science and Marine Environment, Universiti Malaysia Terengganu,
21030 Kuala Nerus, Terengganu, Malaysia
[2]Faculty of Chemical Engineering & Technology, Universiti Malaysia Perlis,
02100, Arau, Perlis, Malaysia
[3]Institute of Climate Adaptation and Marine Biotechnology, Universiti Malaysia Terengganu,
21030 Kuala Nerus, Terengganu, Malaysia
[4]Centro de Química Inorgánica (CEQUINOR, UNLP, CONICET-CCT La Plata),
Facultad de Ciencias Exactas, Universidad Nacional de La Plata,
Bv 120 N° 1465, La Plata 1900, Argentina
[*]Corresponding author: wmkhairul@umt.edu.my

Received: 5 August 2025; **Accepted:** 10 October 2025; **Published:** 14 October 2025

ABSTRACT

The incorporation of alkoxy-substituted chain into thiourea moiety has attracted considerable interest in recent years due to its promising antimicrobial and antibacterial activities, making them potential candidates for antifouling applications. In this study, two new alkoxy-substituted thiourea derivatives, namely; N-(4-(octyloxy)phenyl)-N'-(4-trifluoromethylbenzoyl)thiourea (**3a**) and N-(4-(octyloxy)phenyl)-N'-(4-cyanobenzoyl)thiourea (**3b**) were designed, synthesized, and evaluated for antifouling properties. The compounds were structurally and physicochemical haracterized using ^{1}H and ^{13}C NMR spectroscopy, Fourier Transform Infrared (FTIR) spectroscopy, UV–visible spectroscopy, and thermogravimetric analysis (TGA). In turn, antifouling activities were assessed against *Bacillus subtilis*, *Staphylococcus epidermidis*, *Staphylococcus aureus*, and *Escherichia coli* through preventive and detachment assays. Notably, compound **3b** exhibited strong antifouling performance, achieving up to 94.56% biofilm reduction in the preventive assay, due to the presence of the electron-withdrawing cyano (–CN) substituent. These findings highlight the potential of alkoxy-substituted thiourea derivatives as effective antifouling agents, warranting further exploration for use in fouling-release applications.

Keywords: alkoxy-thiourea; anti-fouling; spectroscopic; thermal analysis

1. INTRODUCTION

Marine biofouling known as undesirable attachment of microorganisms, algae, and larger marine life to submerged surfaces in which continues to impose significant economic and environmental burdens on the shipping industry by increasing hull drag, elevating fuel consumption, and consequently boosting greenhouse gas emissions (He et al., 2024). The

current and conventional antifouling materials reliance on toxic organotin compounds such as tributyltin (TBT) delivered high antifouling efficacy but led to severe ecological damage, endocrine disruption, and widespread regulatory bans. Since the International Maritime Organization's ban on TBT in 2008 (Carrier et al., 2023), there has been a concerted shift toward developing non-toxic, environmentally friendly antifouling solutions. Recent advances Vourna et al. (2025) reported a biocide-free antifouling coating applied to naval steel which showed ~99% performance after 50 weeks of immersion under actual marine conditions, while reducing corrosion rates by about 90%. Similarly, Liu et al. (2024) prepared a self-healing silicone-based coating with thiourea linkages and silver nanoparticles which showed over 96% reduction in bacterial adhesion (including *Pseudomonas aeruginosa* and *Staphylococcus aureus*) and suppressed diatom settlement effectively.

Thiourea derivatives, in particular, are promising because they offer multiple functional features, such as, the thiocarbonyl (C=S), potential hydrogen-bond donors (N-H), and substituent modulation (including alkoxy, electron donating groups) which can be tuned to optimize antimicrobial, antibiofilm, and antifouling performance with lower toxicity risk. In this study, two new alkoxy-substituted thiourea derivatives, namely, N-(4-octyloxyphenyl)-N′-(4-trifluoromethylbenzoyl)thiourea (**3a**) and N-(4-octyloxyphenyl)-N′-(4-cyanobenzoyl)thiourea (**3b**) were synthesized and evaluated for antifouling activity against bacterial biofilms, with the aim of optimizing efficacy, hydrophobicity, and environmental compatibility.

2. MATERIALS AND METHODS

2.1. Materials

Chemicals namely alkyl bromide, sodium hydroxide, ammonium thiocyanate, 4-cyanobenzoyl chloride, 4-(trifluoromethyl)benzoyl chloride, and D-(+)-glucose were obtained from Sigma-Aldrich. Potassium carbonate, Nutrient Broth CM001, ethyl acetate, and acetone, and cassimo acid were purchased from Fisher Scientific. Four test strains used in this study were *Bacillus subtilis* (ATCC 11774), *Staphylococcus epidermidis* (ACCT 12228), *Staphylococcus aureus* (ATCC 25923), and *Escherichia coli* (ATCC 11775). All the bacteria strains were obtained from '*Makmal Belangkas'*, Institute of Climate Adaptation and Marine Biotechnology (ICAMB), Universiti Malaysia Terengganu. Each bacterium was sub-cultured and grown on Nutrient Broth over night at 35°C. The overnight cultured strains were diluted into M63 broth media by the ratio 1:100 to perform the antifouling assay.

2.2. Synthesis of 3a and 3b

N-(4-(alkoxy)phenyl)-N′-(4-trifluoromethylbenzoyl)thiourea (**3a**) and (**3b**) were synthesized *via* the reaction of equimolar amounts of 4-(trifluoromethyl)benzoyl chloride (for **3a**) or 4-(cyano)benzoyl chloride (for **3b**), ammonium thiocyanate, and 4-alkoxyaniline (**2a**). Ammonium thiocyanate (0.17 g, 2.26 mmol) was first dissolved in acetone and stirred for approximately 15 min, after which 4-(trifluoromethyl)benzoyl chloride (0.34 mL, 2.26 mmol) was added, and the mixture was stirred for another 30 min. Subsequently, 4-alkoxyaniline (0.50 g, 2.26 mmol) was introduced, and the reaction mixture was refluxed for *ca.* 5 h. The progress and completion of the reaction was monitored by thin-layer chromatography (TLC). After cooling to room temperature, the mixture was treated with ice to induce precipitation, and the solid obtained was recrystallized from methanol to afford the product as a white, cotton-like solids (**3a**: 0.2595 g, 25%) and (**3b**: 0.1533 g, 17%).

2.3. Antifouling Test for Synthesized Alkoxy Substituted Thiourea Derivatives (3a-3b)

In order to study the antifouling properties of synthesized compounds, two types of antifouling mechanism assays were conducted namely preventive and detachment assay. The samples were filled with triplicates in the 96 well plates for different concentration of N-(4-(alkoxy)phenyl)-N'-(4-trifluoromethylbenzoyl) thiourea **3a** and N-(4-(alkoxy)phenyl)-N'-(4-cyanobenzoyl) thiourea **3b**. The compounds were diluted by two-fold serial dilution from 0.625 mg/mL to 10 mg/mL. For the preventive assay, the diluted samples were loaded into the 96 well plate for each concentration and were incubated for one hour. After one hour of incubation, bacteria strains were injected into the well and incubated overnight. The media and the unattached bacteria cells were discharged by turning the plate over and shaking out the liquid. The plates were then gently rinsed with distilled water (Feoktistova et al., 2016). Crystal violet assay was used for the staining of the bacterial attachment. The quantitative study was performed by using GloMax-Multi detection System at 600 nm. The absorbance in the plate was measured. The difference in procedure of detachment assay with preventive assay was the sequence of samples added. For detachment assay, the samples were added after the overnight incubation of the bacteria strains. All the apparatus and broth that used in the study were sterile by autoclaving at 121°C for 15 minutes. The positive control was incubated with ampicillin while negative control is bacterial incubation without samples. The percentages of the reduction of biofilm were calculated using the formula stated in Eq. 1.

$$\% \text{ of biofilm reduction} = \frac{[(OD_{control})-(OD_{blank})]-[(OD_{sample})-(OD_{blank})]}{(OD_{control})-(OD_{blank})} \times 100\% \quad \text{Eq. 1}$$

3. RESULTS AND DISCUSSION

3.1. Fourier Transform Infrared Spectroscopy (FT-IR)

The synthesized compounds, including precursors, namely N-(4-(octyloxy)phenyl)acetamide (**1a**) (Khairul et al., 2017), 4-octyloxyaniline (**2a**) (Khairul et al., 2017), N-(4-(octyloxy)phenyl)-N′-(4-trifluoromethylbenzoyl)thiourea (**3a**), and N-(4-(octyloxy)phenyl)-N′-(4-cyanobenzoyl)thiourea (**3b**) were characterized using infrared (IR) spectroscopy. Generally, there were five absorption bands of interest namely ν(N–H), ν(C–H), ν(C=O), ν(C–N) and ν(C=S) for the synthesized compounds **1a-3b**. The data were observed in the range of 400 cm^{-1} to 4000 cm^{-1} with different intensities from weak, moderate to strong intensities. The overlay infra-red spectra are shown in Figure 1. Based on the data of the acetamide **1a**, the absorption band at 3233.58 cm^{-1} was observed due to the present of the secondary amine, ν(N–H). Besides, carbonyl functional group shows a sharp absorption band for ν(C=O) at 1658.60 cm^{-1}. **1a** also shows absorption band for ν(C–N) and ν(C–O) at 1240.47 cm^{-1} and 1170.15 cm^{-1}, respectively. According to the IR spectrum of aniline, the vibration for amide group of **2a** was much higher than **1a**. Theoretically, primary amides (NH_2) give bands near 3350 cm^{-1} and secondary amine (NH) gives band at about 3300 cm^{-1}. Therefore, based on the results of the infra-red spectra of **1a** and **2a**, the ν(N–H) vibration for 4-octyloxy aniline was assigned at frequency of 3411.04 cm^{-1} while the ν(N–H) vibration for N-(4-(octyloxy)phenyl) acetamide **1a** was assigned at frequency of 3323.58 cm^{-1}. Hence, the increase in the wavenumber indicates the transformation of the functional group from secondary amine to primary amine. Besides, the vibration for carbonyl ν(C=O) was no longer observed for the IR spectrum of **2a** and this shows the absence of the ketone group in **2a**. Apparently, there is elimination of C=O amide functional group in compound (Hamad et al., 2025). Hence, the

differences in the absorbance band between **1a** and **2a** indicate the changes of two functional groups, amide and ketone in the synthesized compound.

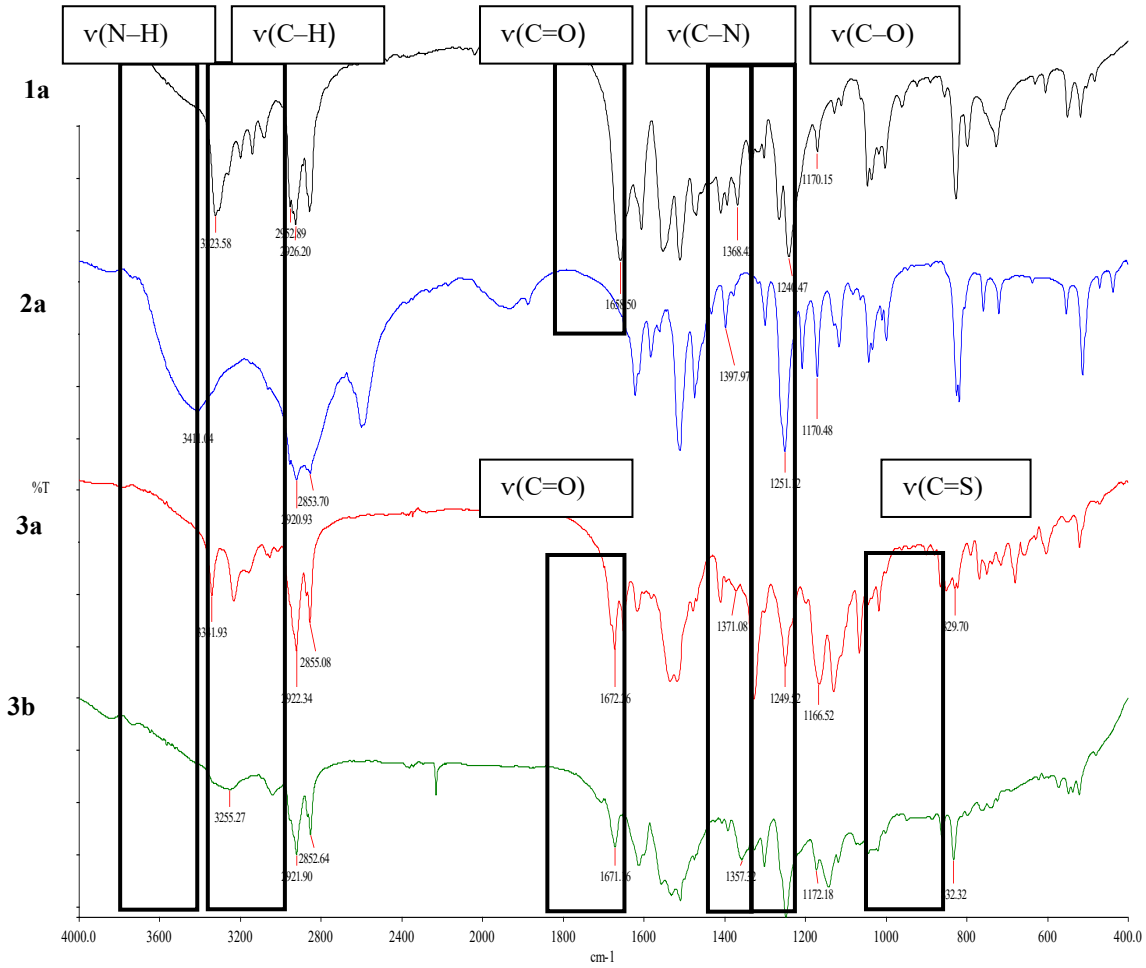

Figure 1. The overlay of all the IR spectra for the synthesized compounds **1a-3b**

Furthermore, the absorption bands for functional group ν(C–N) of **1a-3b** were observed at frequency of 1240.47 cm^{-1}, 1251.12 cm^{-1}, 1249.52 cm^{-1} and 1248.13 cm^{-1}, respectively. According to the data obtained, all the vibration for nitrile was medium absorption intensity. Besides, all synthesized compounds, **1a-3b** perform ν(C–O) vibration in the range of 1166.52-1172.18 cm^{-1}. The wavenumber of the ether functional group was supported by the theoretical expectation where the absorption should be observed in the range of 1350-1000 cm^{-1} (Makhakhayi et al., 2024). Moreover, there were two major absorption bands of interest can be observed in spectra **3a-3b** which were C=S and C=O bands. According to the spectra **3a-3b**, the result shows the strong absorption bands at 1672.26 cm^{-1} and 1671.16 cm^{-1} due to presence of ketone in both compounds. The theoretical frequency for ν(C=O) was slightly higher compared with the result of the study. This may be due to the presence of electron donating phenyl group bonded to the C=O functional group that gives resonance effect to the carbonyl. The statement was strongly agreed by the study of Yiğit et al. (2022) whereby the frequency of the C=O bonds present in acid functional groups were systematically lowered when phenolic groups were close enough to establish hydrogen bonds. Meanwhile, the stretching vibration for ν(C=S) observed in the spectra in **3a-3b** proves that the synthesized compounds were indeed a thiourea compound. According to the study of Qiao et al. (2017), the band appeared in the case of nitrogen containing thiocarbonyl derivatives at the wavelength of 1325 cm^{-1}. However, due to the mixed vibration of N–C=S bond, observation of symmetric CS^{2-} stretching frequencies

was necessary to determine the vibration. In this study, the absorption bands for ν(C=S) in **3a**-**3b** were assigned at 829.70 cm^{-1} and 832.32 cm^{-1} which was parallel to the theoretical result of symmetric stretching vibration at 833-819 cm^{-1}.

3.2. ^{1}H and ^{13}C NMR

All chemical shifts obtained were consistent with previously reported data (Khairul et al., 2015). Several characteristic resonances were observed across all synthesized compounds. A triplet signal appeared in the range of δ_H 0.81-0.82 ppm, corresponding to the methyl protons of the alkoxy group. The methylene protons, labelled H_b, resonated in the δ_H 1.19-1.72 ppm region as multiplet, indicating coupling with adjacent protons. These peaks are characteristic of the long alkoxy chain. In addition, a resonance at δ_H 3.83–3.90 ppm, observed as a triplet, corresponds to the R-O-CH_2 group. For **1a**, a singlet at δ 1.85 ppm was attributed to the methyl group attached to the carbonyl carbon. This signal was absent in **2a**, confirming the loss of the $COCH_3$ functionality. Furthermore, the NMR spectrum of acetamide (**1a**) showed a broad singlet at δ 7.56 ppm, characteristic of an NH proton. In contrast, compound **2a** displayed a broad singlet at δ 10.22 ppm, corresponding to the deshielded protons of the NH_2 group, integrating for two protons (Farzanfar et al., 2015). These observations confirm the conversion of acetamide to aniline. Aromatic proton resonances were observed between δ 6.73-7.96 ppm or all synthesized compounds. Compounds **1a**-**2a** exhibited two pseudo-doublets, whereas **3a**, **3b** showed four pseudo-doublets. In the thiourea derivatives **3a** and **3b**, NH protons adjacent to the carbonyl group resonated at δ 9.07 ppm and δ 9.13 ppm, respectively. Additional broad singlets were detected at δ 12.19 ppm (**3a**) and δ 12.14 ppm (**3b**), attributed to NH protons of the C=S group. These results agree with earlier studies reporting that thiourea compounds typically display two broad absorptions in the downfield region, corresponding to the NHC=O and NH–C=S protons (Sroor et al., 2025).

Table 1. ^{1}H NMR data of all the synthesized compounds

Compounds	Moiety	Chemical Shift, δ_H (ppm)
1a	(t, $^{3}J_{HH}$ = 7 Hz, 3H, CH_3)	0.81
	(m, 12H, 6×CH_2)	1.21–1.7
	(s, 3H, CH_3)	1.85
	(t, $^{3}J_{HH}$ = 6 Hz, 2H, OCH2)	3.83
	(pseudo-d, $^{3}J_{HH}$ = 9 Hz, 2H, C_6H_4)	6.73, 6.76
	(pseudo-d, $^{3}J_{HH}$ = 9 Hz, 2H, C_6H_4)	7.19, 7.30
	(s, 1H, NH)	7.56
2a	(t, $^{3}J_{HH}$= 7 Hz, 3H, CH_3)	0.82
	(m, 12H, 6×CH_2)	1.19–1.69
	(t, $^{3}J_{HH}$= 6 Hz, 2H, OCH_2)	3.83–3.86
	(pseudo-d, $^{3}J_{HH}$ = 9 Hz, 2H, C_6H_4)	6.79, 6.81
	(pseudo-d, $^{3}J_{HH}$ = 9 Hz, 2H, C_6H_4)	7.34, 7.36
	(s, 2H, NH_2)	10.22
3a	(t, $^{3}J_{HH}$ = 7 Hz, 3H, CH_3)	0.82
	(m, 12H, 6×CH_2)	1.19–1.72
	(t, $^{3}J_{HH}$= 6 Hz, 2H, OCH_2)	3.89–3.90
	(pseudo-d, $^{3}J_{HH}$ = 9 Hz, 8H, 2xC_6H_4)	6.86–7.96
	(s, 1H, NH of C=O)	9.07
	(s, 1H, NH of C=S)	12.19
3b	(t, $^{3}J_{HH}$ = 7 Hz, 3H, CH_3)	0.82
	(m, 12H, 6×CH_2)	1.22–1.72
	(t, $^{3}J_{HH}$= 6Hz, 2H, OCH_2)	3.90
	(pseudo-d, $^{3}J_{HH}$ = 9 Hz, 8H, 2×C_6H_4)	6.85–7.96
	(s, 1H, NH of C=O)	9.13
	(s, 1H, NH of C=S)	12.14

Furthermore, ^{13}C NMR spectroscopy was employed to determine both the number and types of carbon atoms present in the synthesized compounds. The spectra were recorded within the δ 0-200 ppm range, with all signals appearing as singlets. The summarized data are presented in Table 2. The observed carbon resonances confirmed the successful synthesis of the target compounds, as all expected signals appeared in their respective regions. The number of signals corresponded to the number of carbons in the aromatic rings, with **3a** and **3b** exhibited additional peaks than **1a** and **2a** due to the presence of an additional aromatic ring (Ali et al., 2025; Naseem et al., 2024). Common characteristic signals across all compounds (**1a**-**3b**) included the methyl (CH_3) group at δ 13.70-13.80 ppm, the R-CH_2 alkoxy group at δ 21.63-30.80 ppm, the CH_2-O ether group at δ 67.28-67.29 ppm, and aromatic carbons at δ 113.70-154.99 ppm.

Table 2. ^{13}C NMR data of all the synthesized compounds

Compounds	Moiety	Chemical Shift, δc (ppm)
1a	(CH_3)	13.07
	(CH_3)	21.63
	(5xCH_2)	23.20–30.79
	(CH_2-O)	67.28
	(C_6H_4)	113.71–154.99
	(C=O)	167.50
2a	(CH_3)	13.07
	(5xCH_2)	21.63–30.78
	(CH_2-O)	67.39
	(C_5H_4)	114.56–123.38
	(C-NH_2)	158.43
3a	(CH_3)	13.07
	(5xCH_2)	21.64–30.80
	(CH_2-O)	67.29
	(12xC_6H_4)	113.70–129.10
	(CF_3)	157.04
	(C=O)	164.57
	(C=S)	177.16
3b	(CH_3)	13.08
	(5xCH_2)	21.64–30.79
	(CH_2-O)	67.29
	(12xC_6H_4)	113.71–134.62
	(CN)	157.09
	(C=O)	164.12
	(C=S)	176.99

For **1a**, a singlet resonance at δ 167.50 ppm confirmed the presence of a carbonyl carbon. In contrast, the ^{13}C NMR spectrum of the corresponding aniline derivative showed no C=O signal; instead, a broad singlet at δ 158.43 ppm was observed, attributable to the NH_2 group. This finding indicates the elimination of the carbonyl functionality and confirms the transformation from amide to amine. In **3a** and **3b**, signals in the ranges of δ 164.12-164.57 ppm and δ 176.99-177.16 ppm were assigned to the carbonyl (C=O) and thiocarbonyl (C=S) carbons, respectively, consistent with previous studies on thiourea derivatives (Shakil et al., 2024; Adam et al., 2016). Additionally, the CF_3 group in **3a** and the CN group in **3b** appeared at δ 157.04 ppm and δ 157.09 ppm, respectively. Nevertheless, the presence of the characteristic N-H signals for thiourea derivatives confirmed the successful synthesis of **3a** and **3b**.

3.3. Thermogravimetric Analysis (TGA)

All synthesized compounds (**1a-3b**) were analyzed using thermogravimetric analysis (TGA), a technique employed to evaluate weight loss and thermal stability. The measurements were carried out under a nitrogen atmosphere at a heating rate of 10°C/min, over the temperature range of 30-800°C. The corresponding thermograms are presented in Figure 2, and the summarized thermal data are provided in Table 3.

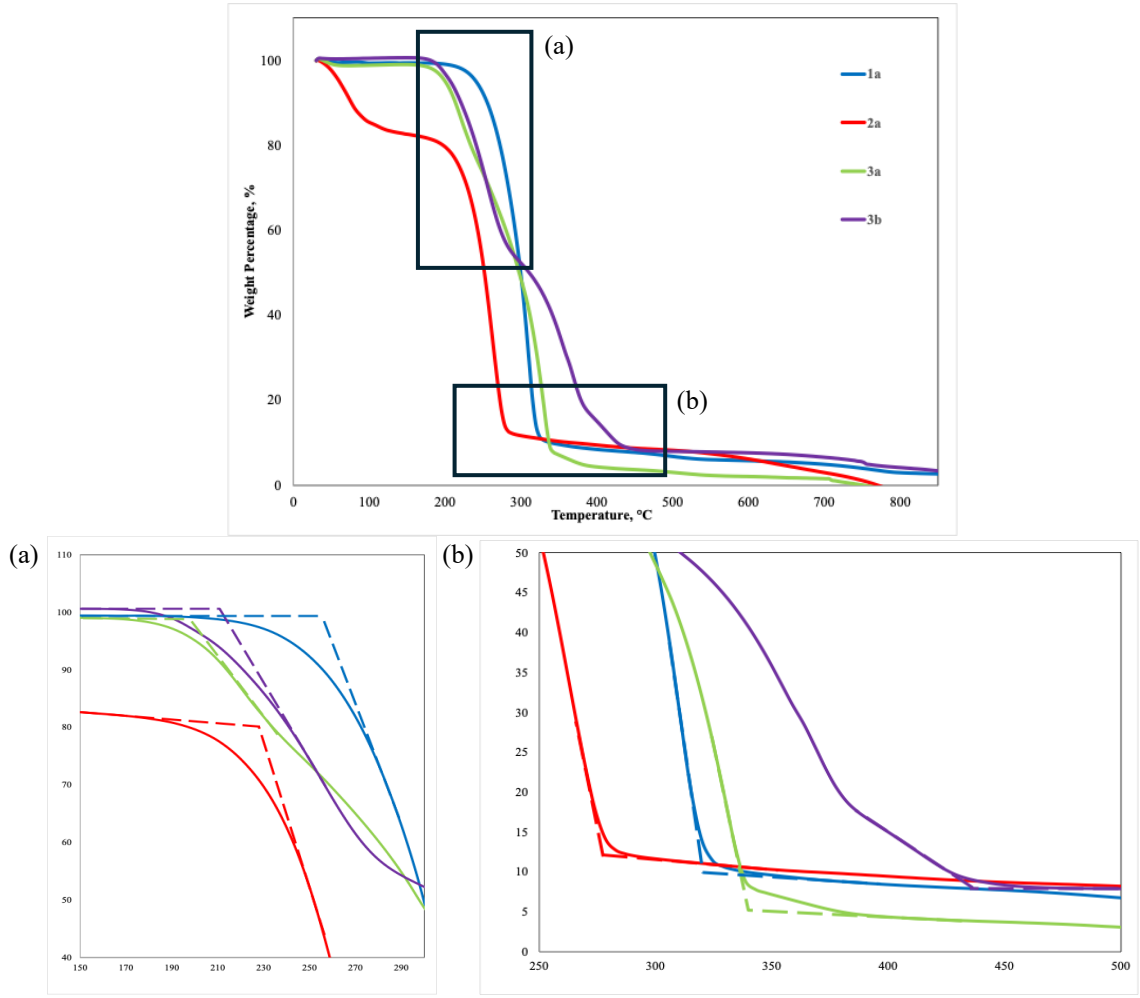

Figure 2. Thermogram for the synthesized compounds **1a-3b** and two highlighted regions shows the (a) onset of degradation, T_{onset} and (b) final degradation stage, T_{offset}

The thermograms of the synthesized compounds revealed two major mass-loss events corresponding to the onset of degradation (T_{onset}) and the final degradation stage (T_{offset}). For all compounds, T_{onset} values were above or near to 200°C, with no detectable mass loss below 100°C, confirming the absence of residual water or solvent (Chowdhury et al., 2025). For sample **2a**, the loss of the weight percentage before 100°C suggests the presence of volatile components. These volatile components could refer to solvent molecules, adsorbed water, or thermally labile functional groups. The results demonstrate that the initial weight loss in compounds **3a** and **3b** near 300°C originates from the cleavage of weak C-N bonds within the thiourea linkage rather than the evaporation of residual volatiles, which distinguishes the thiourea compound degradation profile from the non-thiourea counterparts (Díaz et al., 2017).

In general, compounds **3a** and **3b** exhibited higher T_{onset} values than **1a** and **2a**, indicating superior thermal stability. This enhanced stability can be attributed to the extended conjugation

in the thiourea moiety, suggesting that the thiourea derivatives maintain integrity under elevated temperatures and are suitable for applications requiring prolonged thermal resistance, such as marine antifouling coatings (Nishat & Malik, 2016). Among the synthesized compounds, **3b** demonstrated the highest thermal stability, followed by **3a**, **1a**, and **2a**. Compound **3b** showed the greatest resistance to thermal degradation, as evidenced by its higher T_{offset} value and slower degradation rate. Notably, **3b** did not fully decompose even at 800°C, likely due to trace impurities. In contrast, **3a** underwent complete degradation around 750°C, consistent with higher purity and fewer residual impurities.

Table 3. Data for the thermal analysis of all synthesized compounds

Compounds	T_{onset} (°C)	T_{offset} (°C)
1a	262.14	319.79
2a	228.07	278.51
3a	193.99	338.63
3b	211.21	438.10

3.4. Ultraviolet–visible Spectroscopy (UV-Vis)

According to the UV-Vis results, all synthesized compounds (**1a-3b**) exhibited absorption bands below 300 nm. The important transitions in this study corresponded to the Ar-O-R, Ar-NH_2, C=O, and C=S functional groups. A summary of the spectral data is provided in Table 4, while the corresponding UV-Vis absorption spectra are presented in Figure 3.

Table 4. The electronic adsorption data for synthesized compound

Compounds	λ (nm)	Extinction Coefficient, Ɛ($M^{-1}cm^{-1}$)	Assignments
1a	268.5	20100	π → π*
2a	225.5- 245.50	11100-12100	π → π*
	274.50	6500	n → π*, π → π*
3a	230.00	18600	π → π*
	275.50	13700	n → π*, π → π*
3b	242.0	11800	π → π*
	276.50	8300	n → π*, π → π*

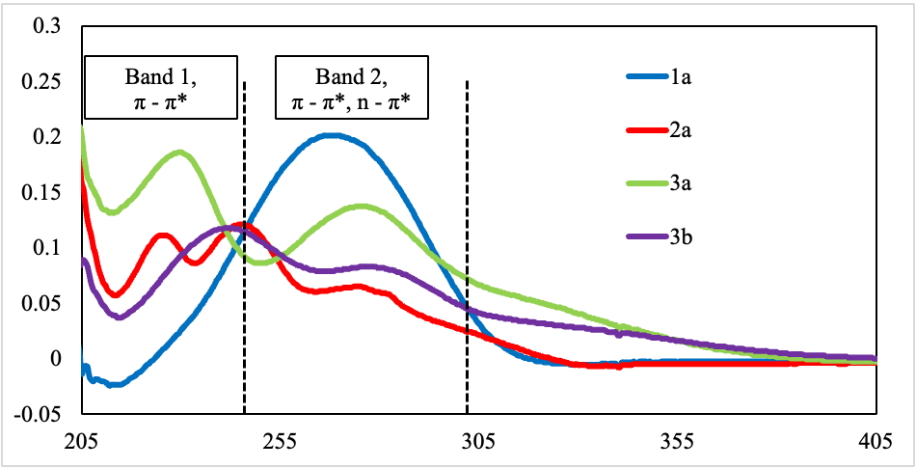

Figure 3. UV-Vis spectra for compounds **1a-3b**

For **1a**, extinction coefficient spectrum showed absorption maxima at λ_{max} 268.5 nm was attributed to the C=O ketone group, corresponding to a π→π* transition. In the case of aniline, a broad absorption band spanning at λ_{max} 225.5–245.5 nm and λ_{max} 274.5 nm, arising from electronic transitions associated with the amine and ether groups, respectively. For **2a,** the

spectrum displayed n→π* transitions from the Ar-NH_2 group and both n→π* and π→π* transitions from the Ar-O-R chromophores. The absence of a C=O absorption band in **2a** confirmed the loss of the ketone functionality and its successful conversion from amide to aniline. Similarly, **3a** and **3b** exhibited absorption bands characteristic of C=O and C=S groups in the ranges of λ_{max} 230.0–242.0 nm and λ_{max} 275.5–276.5 nm, respectively. These findings are consistent with earlier reports by Khairul et al. (2014), who observed C=O and C=S absorptions for thiourea derivatives in the ranges of 232.0–233.6 nm and 256.2–260.0 nm. Moreover, a band near 250 nm was attributed to a transition between the bonding and antibonding orbitals of the C=S group. Collectively, these spectral changes confirm the successful transformation of aniline into the corresponding thiourea derivatives.

3.5. Antifouling Characteristics of the Synthesized Compounds

To evaluate the antifouling potential of the synthesized compounds, the final targeted derivatives **3a** and **3b** were tested against selected bacterial strains. Their activity was assessed through preventive and detachment assays using four representative species: *Bacillus subtilis*, *Staphylococcus epidermidis*, *Staphylococcus aureus*, and *Escherichia coli*. Biofilm formation was quantified using a crystal violet microtiter plate assay, in which 96-well plates served as culture vessels. After staining, biofilm biomass was measured spectrophotometrically at 600 nm using the GloMax-Multi Detection System. The crystal violet assay is widely applied in biofilm studies due to its simplicity, sensitivity, and ability to provide rapid quantitative data on cell viability (Feoktistova et al., 2016). Stained wells were washed to remove unbound dye, and the decolorized product was transferred to a new microtiter plate for optical density (OD) measurement, ensuring optimized results (Idora et al., 2015). This method enabled reliable evaluation of the irreversible attachment of biofilms formed under simulated marine conditions. Compounds were tested at concentrations ranging from 10 mg/mL to 0.625 mg/mL. Ampicillin served as the positive control, while acetone was used as the negative control. Biofilm reduction percentages were calculated and expressed as mean values, with results summarized in Figure 4 and 5, representing preventive and detachment assays, respectively.

The results demonstrated that the detachment assay exhibited significantly higher biofilm reduction compared to the preventive assay. The difference may be attributed to surface activity in the detachment assay, the compounds act directly on preformed biofilms and detached bacterial cells, whereas in the preventive assay, they serve primarily as a protective surface layer to inhibit initial bacterial attachment. Therefore, the preventive assay provides a more realistic simulation of antifouling performance when such compounds are applied to surfaces like ship hulls to prevent marine biofilm growth. Both **3a** and **3b** demonstrated good antifouling activity, particularly at higher concentrations (10-2.5 mg/mL). Biofilm biomass was significantly reduced at 10 mg/mL and 5 mg/mL, although inhibitory effects were markedly lower at very low concentrations, where biofilm reduction did not exceed 50%. These results suggest that the antifouling efficiency of both compounds increases proportionally with concentration (Pereira et al., 2024; Qiu et al., 2022).

Among the tested bacteria, *S. aureus* and *B. subtilis* were most affected. In the preventive assay, compound **3a** achieved a maximum inhibition of 76.17% against *B. subtilis*, while compound **3b** reached 94.56%. In the detachment assay, biofilm reduction was 62.16% for 3a and 79.89% for **3b**. Since antifouling activity above 40% is considered significant, both compounds showed meaningful inhibition, with **3b** consistently outperforming **3a**. The stronger activity of **3b** may be attributed to its structural features, and importantly, it did not promote bacterial growth even at higher concentrations. By contrast, *S. aureus* showed only moderate inhibition, likely due to its non-motile nature and limited ability to form biofilms at the air-water interface. At very low concentrations, both **3a** and **3b** occasionally yielded 0% or negative

values, indicating induced biofilm formation. This may result from bacterial interactions with impurities present in the compounds or limitations of the microtiter plate and crystal violet assay, which can introduce variability. Potential errors include compound loss during successive assay steps, solubility issues influenced by extraction solvents, and uneven distribution or thickness of biofilms, since OD measurements capture only a single point within each well.

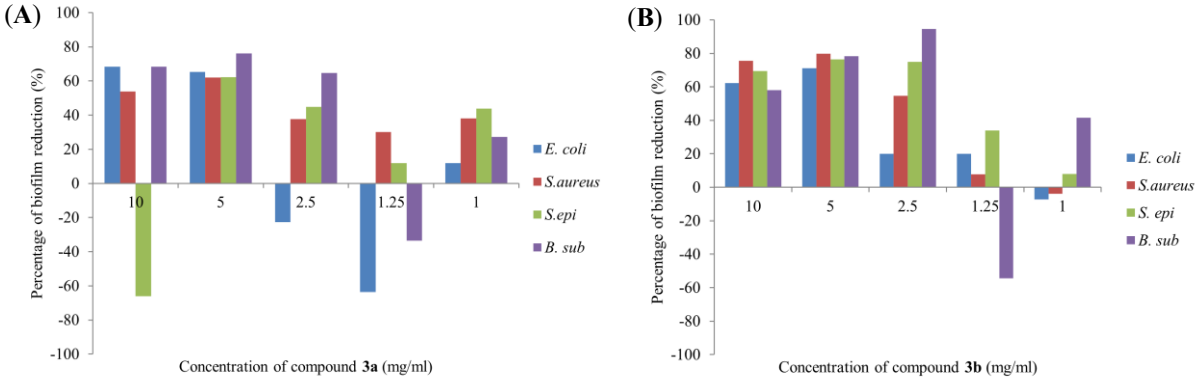

Figure 4. Preventive assay of compound (**A**) **3a**, (**B**) **3b**

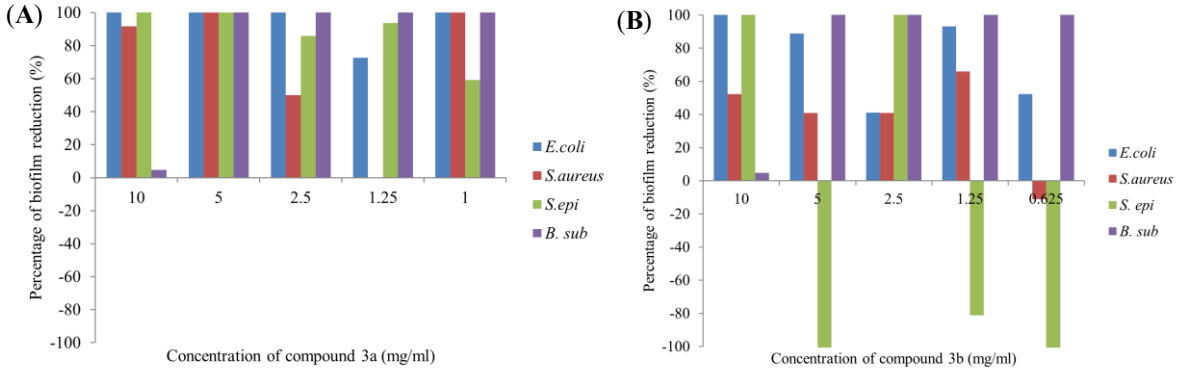

Figure 5. Detachment assay of compound (**A**) **3a**, (**B**) **3b**

Overall, the superior antifouling performance of compound **3b**, bearing a cyano (-CN) group, compared to compound **3a**, which carries a trifluoromethyl (-CF_3) substituent, can be rationalized by their distinct electronic and physicochemical characteristics. Both substituents are electron-withdrawing; however, the cyano group exerts a stronger inductive effect due to its high electronegativity and polarizable triple bond (Scheiner, 2020). This polarization enhances intermolecular interactions between compound **3b** and bacterial cell membranes or biofilm components, facilitating stronger surface activity and biofilm detachment. In contrast, the trifluoromethyl group in **3a**, while also electron-withdrawing, exhibits high lipophilicity that increases its affinity for non-polar environments (O'Hagan, 2008; Purser et al., 2008).

The trifluoromethyl group is bulky and there is the strong C-F bonds create a more rigid molecular structure that may reduce conformational flexibility needed for optimal interaction with bacterial surfaces. Moreover, the cyano group's linear geometry and smaller size allow for better molecular packing and penetration into biofilm matrices compared to the sterically demanding trifluoromethyl substituent (Shabir et al., 2023). The combination of enhanced electronic polarization, optimal lipophilic balance, and favourable steric properties in compound **3b** likely contributes to its higher biofilm inhibition and detachment efficiency under marine conditions where hydrophobic surfaces deter biofilm adhesion.

4. CONCLUSION

In this study, two alkoxy-substituted thiourea derivatives, namely, N-(4-(octyloxy)phenyl)-N′-(4-trifluoromethylbenzoyl)thiourea (**3a**) and N-(4-(octyloxy)phenyl)-N′-(4-cyanobenzoyl)thiourea (**3b**) were successfully synthesized, structurally characterized, and evaluated as potential antifouling agents. The synthetic pathway involved the preparation of precursors N-(4-(octyloxy)phenyl)acetamide (**1a**) and 4-octyloxyaniline (**2a**), followed by the formation of the thiourea derivatives (**3a** and **3b**). All compounds (**1a**-**3b**) were comprehensively characterized using ^{1}H and ^{13}C NMR, FT-IR, UV-Vis spectroscopy, and Thermogravimetric Analysis. The characterization data confirmed the successful synthesis of the target compounds with the expected structural features. Notably, the thiourea derivatives demonstrated excellent thermal stability, maintaining integrity at elevated temperatures, which highlights their suitability for application in marine environments subjected to prolonged thermal stress. Biological evaluation revealed that both **3a** and **3b** displayed significant antifouling activity, particularly at higher concentrations (10 and 5 mg/mL), effectively reducing biofilm formation in *B. subtilis*, *S. aureus*, and *E. coli*, though with limited activity against *S. epidermidis*. Among the tested derivatives, **3b** exhibited the highest biofilm inhibition, achieving up to 94.56% reduction in the preventive assay. Overall, these findings demonstrate that alkoxy-substituted thiourea derivatives, especially for **3b**, possess strong potential as next-generation antifouling agents. The study successfully achieved its objectives, providing a foundation for future development and optimization of thiourea-based coatings for marine applications.

Conflict of Interest
The authors declare no conflicts of interest.

Author Contribution Statement
Sze Ee Sylvia Voon: Writing original draft, Visualization, Data curation, Methodology. Adibah Izzati Daud: Writing, review & editing, Wan M. Khairul: Validation, Supervision, Software, Resources, Project administration, Funding acquisition. Noraznawati Ismail: Conceptualization, Resources, Methodology, Data curation Chiong Hwee Hii: Validation, Writing, review & editing. Mauricio F. Erben: Validation, Writing, review & editing.

Data Availability Statement
The authors confirm that the data supporting the findings of this study are available within the article.

Acknowledgement
The authors would like to acknowledge Universiti Malaysia Terengganu for research facilities and supports as well as assistantship for Sze Ee Sylvia Voon's bachelor's degree final year project.

REFERENCES

Adam F, Fatihah NN, Ameram N, Subramaniam S, Mubarrakh SA. (2016). The synthesis and characterisation of 2-methyl-N-((4-methylpyridine-2-yl) carbamothiol) benzamide: Its preparation with antibacterial study. *Journal of Physical Science*, 27(2), 83-101. doi:10.21315/jps2016.27.2.7

Ali MA, Kutlu E, Altınkaya R, Yavuz O, Emen FM. (2025). Antibacterial activity of hexagonal boron nitride modified with thiourea derivative. *Journal of Molecular Structure*, 142928. doi:10.1016/j.molstruc.2025.142928

Carrier AJ, Carve M, Shimeta J, Walker TR, Zhang X, Oakes KD, Jha KC, Charlton T and Stenzel MH. (2023). Transitioning towards environmentally benign marine antifouling coatings. *Frontiers in Marine Science*, 10, 1175270. doi:10.3389/fmars.2023.1175270

Chowdhury A, Majumdar D, Dutta M, Bhattacharya SK. (2025). Comparative photoelectrochemical study of oligomeric S-Heptazines nanomaterials derived from partial thermal decompositions of urea & thiourea precursors. *Materials Today Catalysis*, 10, 100112. doi:10.1016/j.mtcata.2025.100112

Díaz M, Palop JA, Sanmartín C, Lizarraga E. (2017). Thermal stability and decomposition of urea, thiourea and selenourea analogous diselenide derivatives. *Journal of Thermal Analysis and Calorimetry*, 127, 1663-1674. doi:10.1007/s10973-016-5645-x

Farzanfar J, Ghasemi K, Rezvani AR, Delarami HS, Ebrahimi A, Hosseinpoor H, Eskandari A, Rudbari HA, Bruno G. (2015). Synthesis, characterization, X-ray crystal structure, DFT calculation and antibacterial activities of new vanadium (IV, V) complexes containing chelidamic acid and novel thiourea derivatives. *Journal of Inorganic Biochemistry*, 147, 54-64. doi:10.1016/j.jinorgbio.2015.02.007

Feoktistova M, Geserick P, Leverkus M. (2016). Crystal violet assay for determining viability of cultured cells. *Cold Spring Harbor Protocols*, 4, 87379. doi:10.1101/pdb.prot087379

Hamad AR, Ahmed KM, Omer RA, Azeez YH, Kareem RO, Othman KA, Amin AA. (2025). Synthesis, characterization and computational study of thiourea-based dihydropyrimidine derivatives: A focus on adsorption and reactivity. *Journal of Molecular Structure*, 1325, 140950. doi:10.1016/j.molstruc.2024.140950

He G, Li H, Zhao Z, Liu Q, Yu J, Ji Z, Ning X, Ning F. (2024). Antifouling coatings based on the synergistic action of biogenic antimicrobial agents and low surface energy silicone resins and their application to marine aquaculture nets. *Progress in Organic Coatings*, 195, 108656. doi:10.1016/j.porgcoat.2024.108656

Idora MN, Ferry M, Nik WW, Jasnizat S. (2015). Evaluation of tannin from Rhizophora apiculata as natural antifouling agents in epoxy paint for marine application. *Progress in Organic Coatings*, 81, 125-131. doi:10.1016/j.porgcoat.2014.12.012

Khairul WM, Goh YP, Daud AI, Nakisah MA. (2017). Cytotoxicity effects of alkoxy substituted thiourea derivatives towards *Acanthamoeba* sp. *Arabian Journal of Chemistry*, 10(4), 532-538. doi:10.1016/j.arabjc.2015.05.011

Khairul WM, Mokthar KA, Isa MIN, Samsudin AS, Adli HK, Ghazali SR, Daud AI. (2014). Synthesis and characterization of nitrobenzoylthiourea derivatives as potential conductive biodegradable thin films. *Phosphorus, Sulfur, and Silicon and the Related Elements*, 189(5), 640-651. doi:10.1080/10426507.2013.844137

Makhakhayi L, Malan FP, Senzani S, Tukulula M, Davison C, De la Mare JA, Manicum ALE. (2024). Synthesis, characterisation, X-ray diffraction and biological evaluation of new thiourea derivatives against *Mycobacterium tuberculosis* and cervical cancer. *Journal of Molecular Structure*, 1314, 138818. doi:10.1016/j.molstruc.2024.138818

Naseem S, Oneto A, Ullah S, Fatima S, Mali SN, Jawarkar RD, Khan A, Alharthy RD, Kashtoh H, Al-Haraasi A., Shafiq Z, Boshta NM. (2024). Synthesis, biological evaluation, and molecular modelling of substituted thiazolyl thiourea derivatives: A new class of prolyl oligopeptidase inhibitors. *International Journal of Biological Macromolecules*, 275, 133571. doi:10.1016/j.ijbiomac.2024.133571

Nishat N, Malik A. (2016). Synthesis, spectral characterization thermal stability, antimicrobial studies and biodegradation of starch–thiourea based biodegradable polymeric ligand and its coordination complexes with [Mn (II), Co (II), Ni (II), Cu (II), and Zn (II)] metals. *Journal of Saudi Chemical Society*, 20, 7-15. doi:10.1016/j.jscs.2012.07.017

O'Hagan, D. (2008). Understanding organofluorine chemistry. An introduction to the C–F bond. *Chemical Society Review*., 37(2), 308–319. doi.org/10.1039/b711844a

Pereira S, Oliveira IB, Sousa ML, Gonçalves C, Preto M, Turkina MV, Vasconcelas V, Campos A, Almeida JR. (2024). Antifouling activity and ecotoxicological profile of the cyanobacterial oxadiazine nocuolin A. *Chemosphere*, 365, 143318. doi:10.1016/j.chemosphere.2024.143318

Purser S, Moore PR, Swallow S, Gouverneur V. (2008). Fluorine in medicinal chemistry. *Chemical Society Review*, 37(2), 320-330. doi.org/10.1039/b610213c

Qiao L, Huang J, Hu W, Zhang Y, Guo J, Cao W, Miao K, Qin B, Song J. (2017). Synthesis, characterization, and in vitro evaluation and in silico molecular docking of thiourea derivatives incorporating 4-(trifluoromethyl) phenyl moiety. *Journal of Molecular Structure*, 1139, 149-159. doi:10.1016/j.molstruc.2017.03.012

Qiu H, Feng K, Gapeeva A, Meurisch K, Kaps S, Li X, Yu L, Mishra YK, Adelung R, Baum M. (2022). Functional polymer materials for modern marine biofouling control. *Progress in Polymer Science*, 127, 101516. doi:10.1016/j.progpolymsci.2022.101516

Scheiner, S. (2020). Versatility of the cyano group in intermolecular interactions. *Molecules*, 25(19), 4495. doi.org/10.3390/molecules25194495

Shabir G, Saeed A, Zahid W, Naseer F, Riaz Z, Khalil N, Muneeba, Albericio F. (2023). Chemistry and pharmacology of fluorinated drugs approved by the FDA (2016-2022). *Pharmaceuticals*, 16(8), 1162-1162. doi.org/10.3390/ph16081162

Shakil MA, Ullah S, Halim SA, Mahmood K, Hanif M, Khalid M, Hussain A, Khan F, Altaf AA, Rashid M, Khan A, Anwar MU, Al-Harrasi A. (2024). Synthesis and characterization of some novel benzoyl thioureas as potent α-glucosidase inhibitors: In vitro and in silico. *Journal of Molecular Structure*, 1308, 138133. doi:10.1016/j.molstruc.2024.138133

Sroor FM, El-Sayed AF, Abdelraof M. (2025). Design, synthesis, and antimicrobial activity of new thiourea-uracil derivatives: Anti-biofilm, ROS, DHFR, computational and SAR studies. *Bioorganic Chemistry*, 108719. doi:10.1016/j.bioorg.2025.108719

Yiğit M, Celepci DB, Taslimi P, Yiğit B, Cetinkaya E, Özdemir İ, Gülçin İ. (2022). Selenourea and thiourea derivatives of chiral and achiral enetetramines: Synthesis, characterization and enzyme inhibitory properties. *Bioorganic Chemistry*, 120, 105566. doi:10.1016/j.bioorg.2021.105566